252 *Biochemistry* **2010,** *49,* 252–258
DOI: 10.1021/bi9012676

BIOCHEMISTRY
including biophysical chemistry & molecular biology
Article

Reticulon RTN1-C_{CT} Peptide: A Potential Nuclease and Inhibitor of Histone Deacetylase Enzymes

Ridvan Nepravishta,[‡] Alessia Bellomaria,[‡] Francesca Polizio,[§] Maurizio Paci,[‡] and Sonia Melino*[,‡]

[‡]*Department of Sciences and Chemical Technologies and* [§]*Department of Biological Sciences, University of Rome "Tor Vergata", Rome, Italy*

Received July 24, 2009; Revised Manuscript Received November 6, 2009

ABSTRACT: RTN1-C protein is a membrane protein localized in the ER and expressed in the nervous system, and its biological role is not completely clarified. Our previous studies have shown that the C-terminal region of RTN1-C, corresponding to the fragment from residues 186 to 208, was able to bind the nucleic acids and to interact with histone deacetylase (HDAC) enzymes. In the present work the properties of the synthetic RTN1-C_{CT} peptide corresponding to this region were studied with relation to its ability to bind the metal ions in its N-terminal region. RTN1-C_{CT} peptide is characterized by the presence of high-affinity copper and nickel ion sites. The nuclease activity of the metal−peptide complex was observed due to the presence of an ATCUN-binding motif. Moreover, the effect of the Cu/Ni−RTN1-C_{CT} complexes on the HDAC activity was investigated. The histone deacetylase inhibitors are a new class of antineoplastic agents currently being evaluated in clinical trials. Our data show that the acetylated form of the metal−peptide complex is able to inhibit the HDAC activity at micromolar concentrations. These results allow to propose the Cu/Ni−RTN1-C_{CT} complexes as models for the design of antitumor agents.

The members of the reticulon (RTN)[1] family have been originally classified as markers of neuroendocrine differentiation (*1*); four related metazoan members (Rtn1−4) and alternatively spliced versions have been found (*2*, *3*). RTN1-C is a splice variant produced by the *rtn1* gene (*4*) and in the particular RTN1-C, together with RTN1-A, has been proposed as a molecular marker for diagnosis of neuropathies (*5*). Although it has been demonstrated the implication of the reticulon family in many biological processes, such as axonal regeneration (*6*) and formation of viral replication complex (*7*), the functions of these proteins are still largely elusive. It is notable that recent studies have suggested the involvement of RTN proteins in nuclear pore formation and for the stabilization of nascent pore membrane curvature during nuclear pore complex biogenesis (*8*). In the last years it has been observed that RTN1-C is able to interact with different proteins (*9*, *10*), suggesting the involvement of this reticulon protein in several physiologic functions from apoptosis induction to membrane vesicle trafficking. On the basis of the protein−protein interaction studies it has been possible to hypothesize some of physiological functions of this protein, but the molecular interactions of the external regions of this membrane protein remain still to be elucidated. In our previous studies, we have demonstrated a high ability of the C-terminal fragment of RTN1-C to bind nucleic acids and to interact and inhibit the histone deacetylase 8 enzyme (HDAC8) *in vitro* (*11*). Furthermore, the acetylation of RTN1-C protein *in vivo* was also demonstrated such as the importance of the C-terminal region of the protein in this posttranslational modification, suggesting that the physiological function of RTN1-C can be regulated *in vivo* by the histone acetyltransferase (HAT)−HDAC system (*12*). In fact, the acetylation deeply affects either the metabolic stability or the biological function of the modified proteins and, such as the phosphorylation, it is a posttranslational mechanism for controlling the protein function. *In vivo* the acetylation status of target proteins is tightly regulated by HATs and HDACs (*13*, *14*), and several cellular processes, such as microtuble function or nuclear import (*15*, *16*), are regulated by this enzymatic system. Alterations in the enzyme controlling histone acetylation and deacetylation have been shown to be a direct mechanism of transformation in some malignancies (*17*).

RTN1-C_{CT} peptide, corresponding to the C-terminal region of RTN1-C from residues 186 to 208, is characterized by the presence of cationic residues and of the H4 histone consensus sequence (PS000047 HISTONE_H4) that raise it the property to bind and condense the DNA. On the basis of these previous data, we investigated on the properties of this peptide and on the possibility to use this peptide either as an artificial nuclease or as a model for the design of HDAC inhibitors. In the last years, there has been a great deal of interest in the design new metal molecules with specific nuclease and enzyme inhibition properties for a wide applicability as laboratory tools and therapeutic agents. The presence of a histidine residue in the third position at the N-terminus of the RTN1-C_{CT} peptide allows the formation of a characteristic binding motif, named ATCUN motif, which gives peptides and proteins the ability to bind the metal ions, such as Cu^{2+} and Ni^{2+} (*18*). Naturally it occurs that the ATCUN motif is present in fragments of albumin (*19*) where it has been

*To whom correspondence may be addressed. Tel: 39-0672594449. Fax: 39-0672594328. E-mail: melinos@uniroma2.it.

[1]Abbreviations: AcRTN1-C_{CT}, acetylated RTN1-C_{CT} peptide; AMC, 7-aminocoumarin; APP, amyloid precursor protein; ER, endoplasmic reticulum; EthBr, ethidium bromide; FID assay, fluorescent intercalator displacement assay; HAT, histone acetyltransferase; HDAC, histone deacetylase; MMPP, magnesium monoperoxyphthalate; NE, nuclear envelope; RTN, reticulons; RHD, reticulon homology domain; SNARE, soluble *N*-ethylmaleimide-sensitive factor attachment protein receptor.

 Published on Web 12/10/2009

demonstrated to bind Cu^{2+} and Ni^{2+} with high affinity, K_D $\sim 1.18 \times 10^{-16}$ M and $K_D \sim 10^{-17}$ M, respectively (*20*, *21*). It has been suggested that peptides with this metal-binding motif may have a higher physiological relevance than merely serving as metal transport sites. In fact, the presence of the ATCUN motif has been related either to the carcinogenesis process or to the *in vitro* suppression of tumors (*22*). Furthermore, several Ni/Cu-ATCUN peptide complexes, in the presence of appropriate coreactants, have also demonstrated the ability to cleave both DNA (*21*, *23*−*25*) and viral RNAs (*26*) and, more recently, to inhibit important enzymes *in vitro* (*27*−*29*). In the light of these recent studies, the ability of the metal−RTN1-C_{CT} complex to inhibit the HDAC activity *in vitro* was here also investigated, demonstrating that the metal−peptide complex is able to inhibit this class of enzyme and may represent a model to design anticancer drugs.

EXPERIMENTAL PROCEDURES

Peptide Synthesis. Synthetic peptides were purchased from Peptide Specialty Laboratories GmBH (Germany) and from Spectra 2000 (Rome, Italy). Analysis of the synthetic peptides by reverse-phase high-performance chromatography (RP-HPLC) and mass spectrometry revealed a purity >98%. The sequences of the peptides used were as follows: RTN1-C_{CT}, NH_2-RTHINTVVAKIQAKIPGAKRHAE-$CONH_2$; AcRTN1-C_{CT}, NH_2-RTHINTVVAKIQAKIPGAK(εAc)RHAE-$CONH_2$.

Spectrophotometric Metal Binding Characterization. The peptides were dissolved in water to a concentration of 0.5 mM. Copper chloride was added in a 1:1 molar ratio with the peptides. The pH of the solution was decreased or raised using 0.1 M HCl or 0.2 M NaOH, respectively, and the solutions were equilibrated at each pH before the spectrophotometric measurements. The stoichiometry of Ni^{2+} binding was measured by monitoring the absorbance from 400 to 800 nm, which showed a λ_{max} of 470 nm characteristic of the DTT−Ni^{2+} complex (*30*), in 10 mM Hepes at pH 7.0. A calibration plot was obtained using 10, 20, 40, 60, and 80 μM $NiCl_2$ at a fixed concentration of 500 μM DTT; the plot was a result of three different measures. The visible spectra of the peptide−metal complexes were acquired on Perkin-Elmer Lambda-Bio 20 double-beam spectrophotometer using a 1 cm path length quartz cell at 26 °C.

Circular Dichroism Studies. CD measurements were performed using a Jasco 600 spectropolarimeter (Jasco, Tokyo, Japan) calibrated with camphorsulfonic acid. CD spectra were obtained between 600 and 300 nm using a path length of 1 cm, a time constant of 1.0 s, a 2 nm bandwidth, and a scan rate of 2 nm/min and at 20 or 50 mdeg sensitivity. The average was corrected by four scans of the solvent. Quartz cells of 0.1−1 cm path length sealed and controlled thermostatically were used for the far- and near-UV CD measurements, respectively. The samples for circular dichroism measurements were prepared at 50 μM peptide. The near-UV CD spectra were recorded at 500 μM RTN1-C_{CT} in 20 mM Tris-HCl buffer, at different pHs and equimolar concentration of $NiCl_2$ or $CuCl_2$.

ESR Measurements. X-band (9.2 GHx) ESR spectra at −150 °C were measured on a spectrometer with 100 kHz field modulation of 0.5 mT. A titration at different molar ratio Cu/peptide (0 and 1) was performed using a solution of 300 μM peptide in 50 mM Hepes buffer, at different pHs from 5.2 to 11.0.

Fluorescent Intercalator Displacement Assay (*FID Assay*). The concentration of pDNA stock solution was determined spectroscopically (*31*), and 3 μg of pDNA was added at 900 μL of EthBr (1.5 μg/mL) in 10 mM Hepes, pH 7.0, buffer and 1.5 μg of Ni−RTN1-C_{CT} was added to the solution with the pDNA−EthBr complex. Fluorescence spectroscopy was carried out with a Perkin-Elmer LS luminescence spectrometer using λ_{ex} = 523 nm, λ_{em} = 535−600 nm, 1 cm path length, 1 mL quartz cuvette, slit with 5 nm.

Plasmid Cleavage. The time courses of the plasmid DNA cleavages were performed using a ratio pDNA:Ni/Cu−peptide complex 1:1 w/w (0.5 μg of pDNA, 4500 base pairs, in a volume of 10 μL for each reaction) in 25 mM Tris-HCl, pH 7.5, sterile buffer filtered. After equilibration of DNA−metal−peptide solutions for 10 min at room temperature, the reactions were initiated by addition of ascorbic acid (1:10 c/c) or MMPP (1:10 c/c) for the Cu− or Ni−peptide complex, respectively. The reactions were carried out at 37 °C and were terminated by addition of 2 μL of 6× gel loading buffer (5% glycerol, 0.125% bromophenol blue, 25 mM EDTA) and placed on ice before electrophoresis in 1% agarose gel in the TAE buffer. Samples were run for 120 min at 70 V and stained with ethidium bromide.

HDAC Inhibition Assay and Oxidative Damage by RTN1-C_{CT} Peptides. Histone deacetylase from rat commercially available (Alexis, Switzerland) was used for the histone deacetylase activity, and α-Boc(εAc)Lys-AMC, also termed MAL (Alexis), was used as the fluorescent histone deacetylase substrate. The assay was performed as previously described (*32*), using 1.4 mM NaH_2PO_4, 18.6 mM Na_2HPO_4, pH 7.9, 0.25 mM EDTA, 10 mM NaCl, 10% (v/v) glycerol, and 10 mM mercaptoethanol as incubation buffer, and the reaction was stopped by addition of 80% CH_3CN and 0.1% TFA. The assay was performed by RP-HPLC chromatography using a Shimadzu HPLC system LC-10ATvp model; the elution of peaks was monitored by RF535 fluorescence detector (excitation wavelength 330 nm, emission wavelength 395 nm) and an Applied Biosystems RP-C18 column (5 μM; 250 × 4.6 mm). The elution was performed using 0.1% TFA (solvent A) and 80% CH_3CN and 0.1% TFA (solvent B) with an eluting gradient 2 min 0% B solvent, 0−50% in 40 min, 50% for 10 min, 50−90% in 5 min at flow rate 0.8 mL/min. Fluorescence HDAC activity assay was performed using Fluor de-Lys, fluorogenic deacetylase substrate, (acetyl)-Arg-His-Lys(ε-acetyl)-Lys-coumarin, according to the manufacturer's instructions (BIOMOL International LP, Plymouth Meeting, PA). Briefly, 0.12−1.12 μM HDAC8 recombinant protein or 0.5 μL of 10 mg/mL HeLa nuclear extract, in 50 mM Tris-HCl, 137 mM NaCl, 2.7 mM KCl, 1 mM $MgCl_2$, pH 8.0, buffer, was used, and the reaction was started by adding 5 μL of substrate solution (100 μM final concentration) at 45 μL of sample solution followed by 60 min of incubation at 37 °C. The reaction was stopped by addition of 50 μL of trypsin/TSA stop solution (10 mg/mL trypsin from porcine pancreas, Sigma-Aldrich, in 100 mM ammonium bicarbonate, pH 8.0, buffer and 2 μM TSA). After a 20 min incubation period at 30 °C, the release of AMC by measuring the fluorescence at 460 nm (λ_{ex} = 360 nm) was monitored. The AMC signals were recorded against a blank with buffer and substrate but without the enzyme. To observe the inhibition effects of the peptides 15 min of preincubation of the enzyme in the presence of them, at room temperature, before the addition of the substrate was performed. Initial velocity (V_0) values were plotted as a function of substrate concentration [S] and fit to the Michaelis−Menten equation, $V_o = V_{max}[S]/([S] + K_m)$, using GraphPad software to obtain K_m values. The inhibition was determined

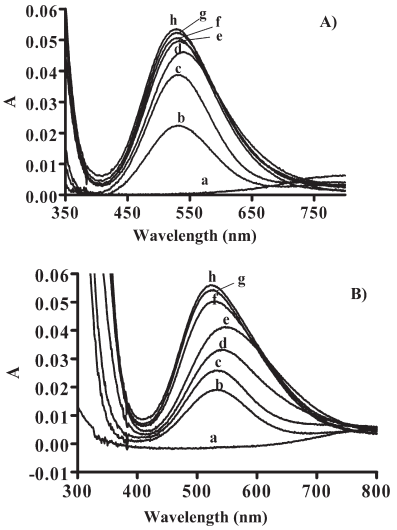

FIGURE 1: UV−vis spectra of (0.5 mM) RTN1-C_{CT} with and without acetylation in the presence of an equimolar concentration of Cu^{2+} at different pHs. (A) RTN1-C_{CT} at pH 3.4 (a), 4.09 (b), 5.09 (c), 7.23(d), 8.48 (e), 9.2 (f), 9.6 (g), and 10.17 (h). (B) AcRTN1-C_{CT} at pH 3.18 (a), 4.35 (b), 5.9 (c), 6.7 (d), 7.7 (e), 8.7 (f), 9.7 (g), and 10.2 (h). The peptide shows the characteristic maximum at 525 nm of the Cu^{2+} bound. We have also performed the metal-binding measures at 37 °C and found that the differences in binding were negligible (< 3%).

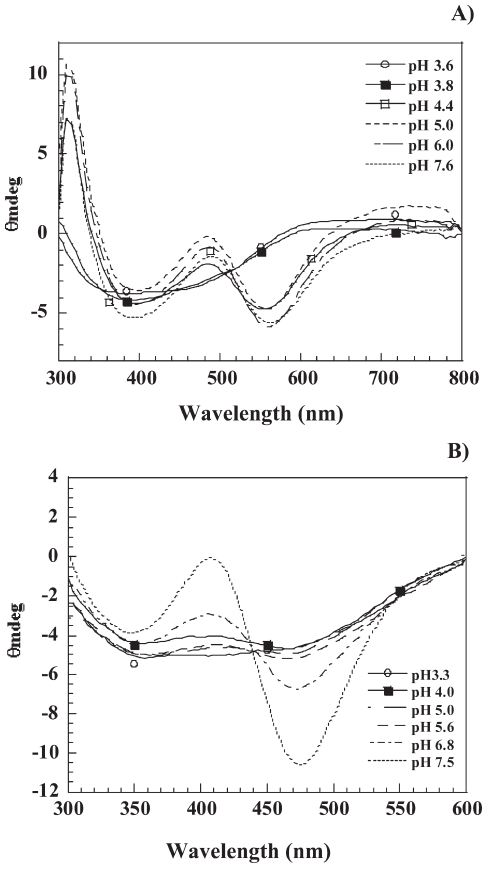

FIGURE 2: Near-UV CD spectra of 0.5 mM Cu−RTN1-C_{CT} at different pHs. (A) Cu−RTN1-C_{CT} at pH 3.5 (a), 4.5 (b), and 6.4 (c). (B) Ni−RTN1-C_{CT} at pH 3.3 (a), 4.0 (b), 5.0 (c), 5.6 (d), 6.8 (e), and 7.5 (f). The measurements were performed at equimolar concentrations of Cu^{2+}/Ni^{2+} and RTN1-C_{CT}.

from Lineweaver−Burk for competitive inhibitors. All experiments were carried out in triplicate. The oxidative damage to the HDAC protein by metal−RTN1-C_{CT} complexes was performed using a molar ratio HDAC8/metal−complex 1:10 c/c, in the same buffer used for the fluorescence HDAC assay (see above), and the oxidative reaction was started by addition of ascorbic acid in a molar ratio metal−complex/ascorbic acid 1:10 c/c at 37 °C.

RESULTS AND DISCUSSION

Metal Binding of RTN1-C_{CT} Peptide. RTN1-C_{CT} peptide is characterized by the presence of a histidine residue in the third position forming a characteristic metal-binding motif, named ATCUN motif, which is able to bind the metal ions, such as Cu^{2+} and Ni^{2+} (*18*). We have performed spectroscopic studies to investigate the ability of the RTN1-C_{CT} peptide to bind Cu^{2+} and Ni^{2+} ions. In Figure 1 are shown the UV−vis spectra of the RTN1-C_{CT} peptide and its acetylated form in the presence of an equimolar concentration of Cu^{2+} ions at different pHs. The peptides showed the characteristic maximum at 525 nm of the Cu binding in the pH range between 3.4 and 10.17. The absorption maximum at 525 nm obtained at a low pH and maintained through a wide range of pH is characteristic of a Cu−ATCUN complex formation (*19*, *33*). Moreover, further structural features of the binding of metals to RTN1-C_{CT} peptide has been obtained by CD studies. CD spectroscopy was performed at different pHs in the presence of an equimolar concentration of Cu^{2+} or Ni^{2+} (see Figure 2). CD spectra in the presence of copper or nickel ions at pHs higher than 4.0 displayed two dichroic bands at 560 and 480 nm in the case of copper and at 480 and 410 nm for the nickel bands, which are characteristic of a distorted square-planar geometry of nickel or copper ions in a Ni/Cu-(II)N4 site involving an histidine residue found for ATCUN metal binding (*34*). ESR spectroscopy of the Cu−RTN1-C_{CT} complex was performed at −150 °C to investigate the presence of Cu^{2+} free in the solution, and ESR spectra of the peptide at 1:1 molar ratio of Cu^{2+}/peptide at different pHs (data not shown) showed that at 1:1 Cu/peptide molar ratio the presence of free Cu^{2+} is not visible and the copper ions were bound to the peptide at physiological pH. The *f* values (= g/l/A/l) were consistent with those of the Cu^{2+}−peptide complex reported by Pogni et al. (*35*), indicating that the complex has a square-planar geometry, which is characteristic of the copper binding of the ATCUN motif (see Supporting Information Figure 2S).

The stoichiometry of Ni^{2+}−RTN1-C_{CT} binding was measured by monitoring the absorbance of the DTT−Ni^{2+} complex at λ_{max} 470 nm in 10 mM Hepes, pH 7.0, buffer (*30*). In Figure 3 are shown the spectra performed for calculating the stoichiometry of the metal binding. The peptide was incubated with $NiCl_2$ in a molar ratio 1:2 c/c (peptide/Ni^{2+}) in 10 mM Hepes, pH 7.0, buffer for 15 min at 26 °C, and then DTT was added at a final concentration of 500 μM. The estimated concentrations of nickel ions free and bound to RTN1-C_{CT} were 52 and 48 μM, respectively (~48% bound), thus showing a characteristic 1:1 binding stoichiometry of the Ni^{2+}−RTN1-C_{CT} complex.

Interaction of the Metal−RTN1-C_{CT} Complex with pDNA. In the previous work we have observed that the RTN1-C_{CT} peptide is able to induce DNA condensation, in time-dependent manner, when the RTN1-C_{CT} peptide was added to the pDNA−EthBr mixture (*11*). The displacement of EthBr from DNA is a direct method of measuring the binding affinity of compounds that lack a chromophore. Fluorescence of free EthBr in solution was strongly quenched by aqueous solvent and exhibited weak fluorescence, and the addition of DNA to the

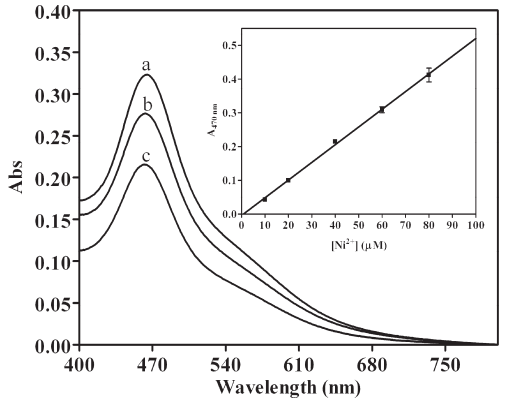

FIGURE 3: Stoichiometry of the Ni−RTN1-C_{CT} complex. RTN1-C_{CT} (50 μM) was incubated with 100 μM $NiCl_2$ (1:2 rate) for 15 min at room temperature in 10 mM Hepes, pH 7.0, and then DTT was added at a final concentration of 500 μM. The calculated stoichiometry for this complex was 1:1. (a) and (c) are the absorbance of 60 and 40 μM Ni^{2+}−DTT; (b) is the absorbance of 100 μM Ni^{2+}−DTT in the presence of 50 μM RTN1-C_{CT}.

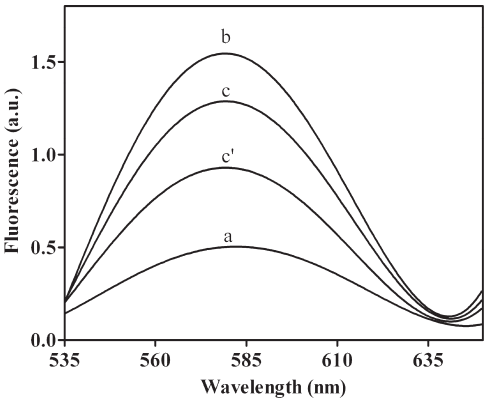

FIGURE 4: Fluorescence intercalator decay assay (FID). Fluorescence spectra of EthBr (1.5 μg/mL) alone (a), in 1 mL of 10 mM Hepes, pH 7.0, in the presence of 3 μg of pDNA (b), and after addition of 30 μg RTN1-C_{CT} (c) or Ni^{2+}−RTN1-C_{CT} (Ni^{2+}/peptide 1:1) (c′) after 3 h at 26 °C.

solution induces a significant fluorescence enhancement due to the DNA binding (*31*). In Figure 4 are shown the results of a FID assay using the metal−RTN1-C_{CT} complex and pDNA. The complex is able to bind the DNA and induce a major condensation of the pDNA than that observed with the peptide alone. The major affinity of the Ni−RTN1-C_{CT} for the pDNA is probably due to the property of the Ni−ATCUN motif to bind the nucleic acids. Previously, in fact, it has been observed that the Ni−ATCUN motif alone is able to bind the DNA at the minor groove of A/T-rich regions and cleave it in the presence of coreactants, such as mild reducing agents (*36*, *23*).

DNA Oxidation by Cu/Ni−RTN1-C_{CT} peptide. In the last years, the design of artificial nucleases has generated great interest; artificial peptidic nucleases could have wide applicability either as tools in molecular biology and therapy or as probes of the structure and function of nucleic acids.

Therefore, considering the high nucleic acid-binding property of RTN1-C_{CT} (*11*) and the ability of the peptide to bind Cu/Ni ions, we also investigated its ability to induce the DNA cleavage. The Ni/Cu−peptide complexes with the ATCUN motif cause DNA cleavage through a mechanism involving C-4′H oxidation and hydroxylation of proteins (*37*, *38*). In our case, a rapid

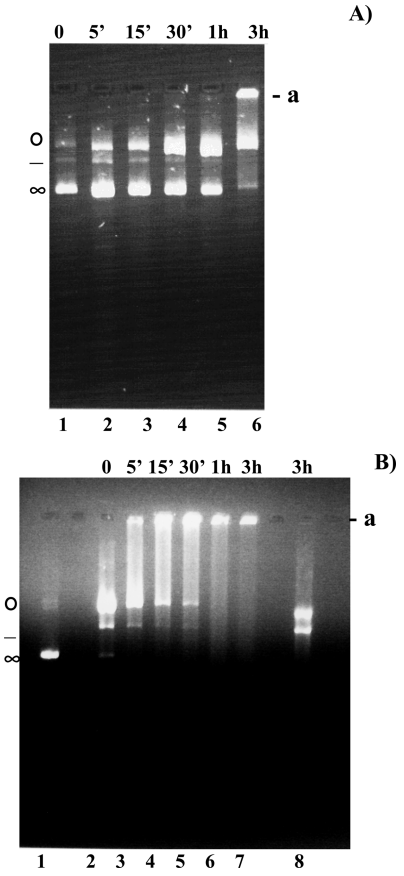

FIGURE 5: Cleavage of pDNA by the metal−RTN1-C_{CT} complex. Agarose gel electrophoresis of pDNA (0.5 μg) in filtered 50 mM Tris-HCl, pH 7.0, buffer with pDNA/metal−RTN1-C_{CT} 1:1 w/w ratio (A) after 0 min, 5 min, 15 min, 30 min, 1 h, and 3 h of incubation at 37 °C in the presence of Cu−RTN1-C_{CT} and ascorbic acid. Cu−RTN1-C_{CT}/ascorbic acid 1:10 molar ratio (B) in the absence (lane 1) and in the presence of Ni−RTN1-C_{CT} after 0 min, 5 min, 15 min, 30 min, 60 min, and 3 h (lanes 2−7) and only in the presence of $NiCl_2$ after 3 h at 37 °C (lane 8). The cleavage was activated by addition of MMPP with a Ni−peptide/MMPP 1:10 molar ratio.

degradation of supercoiled pDNA was observed when the Cu−RTN1-C_{CT} complex was added to pDNA solution in the presence of ascorbate (Figure 5A). Moreover, the appearance of an **a** band, probably due to the formation of a complex between the linear form of pDNA and the Cu−RTN1-C_{CT} complex, was observed for times longer than 1 h. The Cu−RTN1-C_{CT} complex is able to cleave the pDNA in the presence of ascorbate, and in fact, a rapid degradation of the supercoiled pDNA was found to produce nicked pDNA at 37 °C (shown in Figure 5A). Likely to the copper complex also the Ni−RTN1-C_{CT} complex induced a rapid cleavage of the pDNA in the presence of magnesium monoperoxyphthalate (MMPP) (Figure 5B) and a concurrent disappearance of the supercoiled band; the appearance of nicked bands and after 5 min an **a** band on the top of the gel was observable, in agreement with that observed for the Cu−peptide complex. On the contrary, the Ni^{2+} ions alone in the presence of MMPP are not able to induce the formation of the **a** band, and only after 3 h the nicked form of the pDNA was observable. The presence of cationic residues and of the histone H4 consensus sequence in the RTN1-C_{CT} promotes the interaction with the DNA backbone (*11*) enhancing the nuclease effect due to the ATCUN motif. The acetylated forms of the Ni/Cu−peptide complexes were also able to induce an oxidative cleavage of pDNA, but a smaller cleavage was observable due to a lower

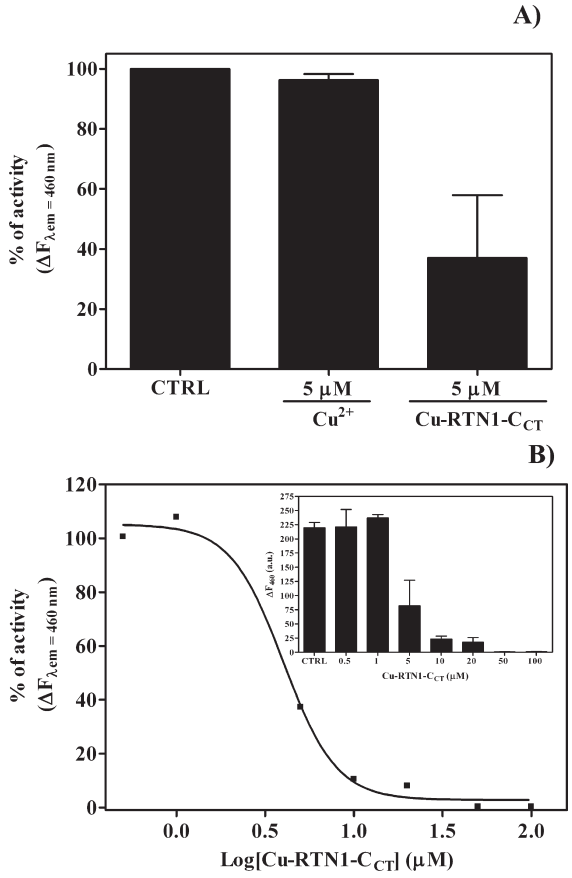

FIGURE 6: Inhibition of HDAC activity by Cu−RTN1-C_{CT}. (A) HeLa nuclear extract HDAC was preincubated with 0.5, 1, 5, 10, 20, 50, and 100 μM Cu^{2+}−RTN1-C_{CT} and 100 μM ascorbic acid for 15 min at room temperature. The assay was performed as described in Experimental Procedures. The calculated IC_{50} was 4 μM. (B) Inhibition of HeLa nuclear extract HDAC. HDAC activity by 5 μM Cu^{2+} alone and Cu−RTN1-C_{CT} in the presence of 50 μM ascorbic acid.

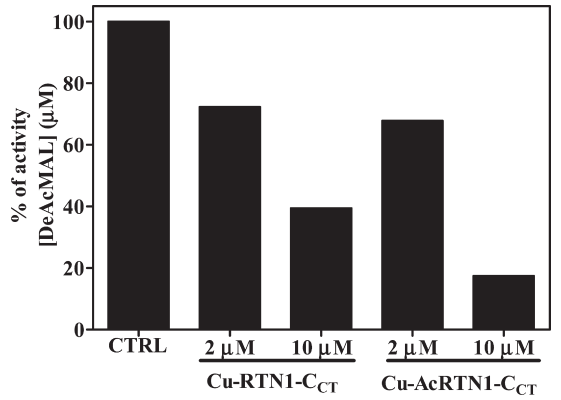

FIGURE 7: HDAC assay by HPLC. HDAC rat (1 unit) was incubated with the indicated concentrations of Cu−RTN1-C_{CT} and Cu−AcRTN1-C_{CT} in the presence of ascorbic acid before the assay.

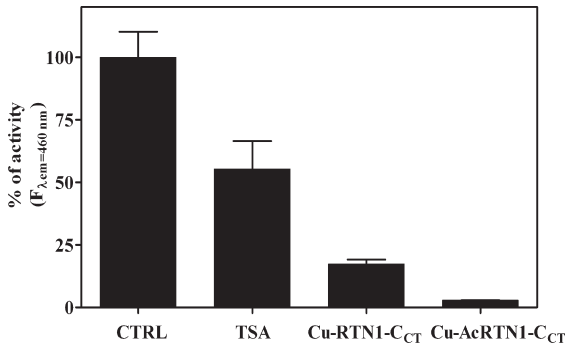

FIGURE 8: Inhibition of HDAC8 activity. 100 nM HDAC8 in the presence of 10 μM ascorbic acid was used as control. The enzyme was incubated for 15 min at room temperature with 1 μM TSA, 100 nM Cu−RTN1-C_{CT}, or Cu−AcRTN1-C_{CT}. All inhibition assays where conducted in the presence of 10 μM ascorbic acid.

capacity of the peptide to interact with DNA, as shown by the absence of the **a** band to the top of the gel (Supporting Information Figure 3SA,B).

Cu−RTN1-C_{CT} Inhibits HDACs. The modifications such as acetylation have functional roles by modulating transcription efficiency (*39*). Acetylation occurs at the ε-amino groups of lysine residues present within the N-terminal extensions of the histones and some nonhistone proteins that have been found transcription factors, heat shock proteins, and structural proteins (*40*). The balance of two families of HATs and HDACs tightly controls the acetylation status of target lysines (*13*, *14*). HDACs catalyze the removing of the acetyl group from the acetyl-lysine residues, and these enzymes were divided into four classes according to phylogenetic analyses and sequence homologies (*41*−*46*). In this work the effects of the metal−peptide complex on the HDAC activity, in the presence of coreactants, were assayed. A loss of the deacetylase activity of the nuclear HeLa extract, in the presence of Cu−RTN1-C_{CT} under oxidative condition, was observed. About 50−60% loss of total HDAC activity was found at 5 μM Cu−RTN1-C_{CT} concentration, whereas free Cu^{2+} under identical conditions brought about only 4% loss of total activity (Figure 6A). In these experiments before adding the substrate, the copper−peptide complex or the copper ions were preincubated with the enzyme for 30 min at room temperature. A dose dependence of the HDAC inhibition by the Cu−RTN1-C_{CT} complex was observed, and a 4.0 ± 2.16 μM IC_{50} value was estimated (Figure 6B). Figure 7 shows the changing of the percentage of HDAC activity of rat enzyme in the presence of metal−peptide complexes. HDAC activity was assayed by HPLC assay using MAL as fluorescent substrate. A decrease of HDAC activity was observed in the presence of either Cu−RTN1-C_{CT} or Cu−AcRTN1-C_{CT} complex and 10 mM ascorbic acid. A high inhibition was observed when the enzyme was preincubated with Cu−peptide before the reaction with MAL substrate. In fact, after 30 min of preincubation at room temperature, with 10 μM Cu−RTN1-C_{CT} or Cu−AcRTN1-C_{CT}, and 90 min of reaction with the substrate approximately inhibition 61% and 82% loss of total HDAC activity were respectively observed (Figure 8). By contrast, under identical condition no HDAC activity inhibition was observed in the presence of ascorbic acid alone; thus all controls were performed in the presence of the same concentration of ascorbic acid. The preincubation of the rat HDACs with the metal−peptide complexes induced a stronger inhibition than that observed in the absence of preincubation (data not shown). The observed difference of inhibition with and without the preincubation could be explained with an interaction of the metal−peptide complex in the active site. In fact, the presence of substrate could inhibit the interaction with the metal−peptide reducing its inhibitor effect. Moreover, the acetylated form was more inhibiting than the other one, suggesting again possible direct interaction of the metal complex close the catalytic site.

Metal−RTN1-C_{CT} Induces Oxidative Damage of HDAC8. Previously, it has been suggested that specific Ni/Cu-ATCUN complexes could inhibit enzyme activity by inducing modification

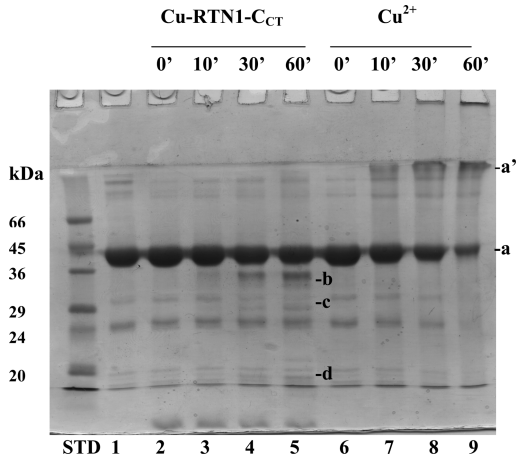

FIGURE 9: HDAC8 interaction with Cu−RTN1-C_{CT} or with $CuCl_2$. SDS−PAGE 12% gel acrylamide of 10 μM HDAC8 in the presence of only 1 mM ascorbic acid (lane 1) after 60 min at 37 °C and in the presence of 100 μM Cu−RTN1-C_{CT} complex (Cu^{2+}:peptide 1:1 c/c) (lanes 2−5) or 100 μM $CuCl_2$ (lanes 6−9) after 0, 10, 30, and 60 min of incubation with 1 mM ascorbic acid at 37 °C.

of active site amino acid residues by reactive oxygen species (*47*, *48*). In fact, many amino acid residues are susceptible to metal-catalyzed oxidation including histidine, arginine, lysine, proline, methionine, and cysteine (*49*). The mechanism of inactivation of HDAC8 by Cu−RTN1-C_{CT} in the presence of ascorbic acid was investigated by SDS gel electrophoresis over a range of incubation times (see Figure 9). After 30 min of incubation in the presence of Cu−RTN1-C_{CT}, a band at about 35 kDa (**b** band) was observable in the SDS−PAGE due to a fragmentation of the HDAC8 enzyme, and this fragmentation was more visible after 60 min of incubation for the presence of other bands. Furthermore, no bands at higher molecular masses were observed, suggesting that the time-dependent loss of enzyme activity could be dependent on the protein cleavage and on the oxidation of the aforesaid residues. The same effect was also observed for the metal complex of the acetylated form in the presence of HDAC8 and ascorbic acid, inducing the formation of a corresponding **b** band after 60 min (see Supporting Information Figure 4S). This result suggests that the higher inhibition effects of the acetylated metal complex could be explained by the oxidation of essential residues that does not lead to additional variations of the molecular mass of the enzyme.

By contrast, a different electrophoretic pattern of the HDAC8 after treatment with $CuCl_2$ and ascorbic acid was observed; in fact, it was characterized by protein bands at high molecular masses due to formation of fragments (**a′** band). Direct characterization of these protein bands by mass spectrometry was precluded by the low concentrations obtained.

CONCLUSIONS

The study of the interaction between metal ions and short peptides having important interaction with other biological macromolecules can be highly useful in designing new molecules with interesting properties and wide applicability as laboratory tools and therapeutic agents.

Nuclease activity of the RTN1-C_{CT} peptide is due to the ATCUN motif, which is present at the N-terminus of the peptide. Ni/Cu-ATCUN peptide complexes were shown to bind and cleave the DNA through an oxidative mechanism in the presence of coreactants. The cationic residues and the H4 consensus sequence present in this peptide allow a better interaction with the DNA backbone enhancing the nuclease effect of the metal-binding motif. Although in the past it has been shown that the Cu/Ni-ATCUN complex is able to mediate protein cleavage and cross-linking (*38*), only in the last years has their potential for enzyme inactivation been demonstrated. The studies herein show that the Cu−RTN1-C_{CT} complex is able to induce a dose-dependent inhibition of HDACs, consistent with an oxidative damage and cleavage to the enzyme. Recently, it has been observed that specific Cu−ATCUN−peptide complexes, which are able to bind angiotensin-converting enzyme (ACE) or thermolysin (TLN), inhibit the enzymatic activity of these enzymes in the presence of ascorbic acid by formation of reactive oxygen species (*27*−*29*). Electrochemical studies supported formation of Cu^{3+} in these metal−peptide complexes, suggesting a mechanism of copper(III)-oxo species as a nondiffusible reactive oxygen species (*29*, *37*). Our studies demonstrate the possibility to use the selective oxidative damage by metal−ATCUN−peptide substrates as a strategy to inhibit the HDAC activity and represent progress toward the development of specific metallopeptides or peptidomimetic inhibitors of this class of enzymes, which are involved in the degenerative diseases.

ACKNOWLEDGMENT

We thank Dr. Stefania Di Marco for giving us the purified HDAC8 enzyme, Prof. Mauro Piacentini for helpful discussion on reticulon proteins, and Dr. Barbara Fazi for assistance in the initial step of the research.

SUPPORTING INFORMATION AVAILABLE

Figure 1S, AcRTN1-C_{CT} and pDNA interaction; Figure 2S, ESR spectrum of the Cu−RTN1-C_{CT} complex; Figure 3S, pDNA cleavage by Cu/Ni−AcRTN1-C_{CT} complexes; Figure 4S, oxidative effect of the Cu−AcRTN1-C_{CT} complex on HDAC8. This material is available free of charge via the Internet at http://pubs.acs.org.

REFERENCES

1. Oertle, T., and Schwab, M. E. (2003) Nogo and its paRTNers. *Trends Cell. Biol. 13*, 187–194.
2. van de Velde, H. J., Roebroek, A. J., Senden, N. H., Ramaekers, F. C., and Van de Ven, W. J. (1994) NSP-encoded reticulons, neuroendocrine proteins of a novel gene family associated with membranes of the endoplasmic reticulum. *J. Cell. Sci. 107* (Part 9), 2403–2416.
3. van de Velde, H. J., Senden, N. H., Roskams, T. A., Broers, J. L., Ramaekers, F. C., Roebroek, A. J., and Van de Ven, W. J. (1994) NSP-encoded reticulons are neuroendocrine markers of a novel category in human lung cancer diagnosis. *Cancer Res. 54*, 4769–4776.
4. Roebroek, A. J., van de Velde, H. J., Van Bokhoven, A., Broers, J. L., Ramaekers, F. C., and Van de Ven, W. J. (1993) Cloning and expression of alternative transcripts of a novel neuroendocrine-specific gene and identification of its 135-kDa translational product. *J. Biol. Chem. 268*, 13439–13447.
5. Dupuis, L., Gonzalez de Aguilar, J. L., di Scala, F., Rene, F., de Tapia, M., Pradat, P. F., Lacomblez, L., Seihlan, D., Prinjha, R., Walsh, F. S., Meininger, V., and Loeffler, J. P. (2002) Nogo provides a molecular marker for diagnosis of amyotrophic lateral sclerosis. *Neurobiol. Dis. 10*, 358–365.
6. Li, Sh., Liu, B. P., Budel, S., Li, M., Ji, B., Walus, L., Li, W., Jirik, A., Rabacchi, S., Choi, E., Worley, D., Sah, D. W. Y., Pepinsky, B., Lee, D., Relton, J., and Strittmatter, S. M. (2004) Blockade of Nogo-66, myelin-associated glycoprotein, and oligodendrocyte myelin glycoprotein by soluble Nogo-66 receptor promotes axonal sprouting and recovery after spinal injury. *J. Neurosci. 24*, 10511–10520.
7. Tang, W. F., Yang, S. Y., Wu, B. W., Jheng, J. R., Chen, Y. L., Shih, C. H., Lin, K. H., Lai, H. C., Tang, P., and Horng, J. T. (2007)

Reticulon 3 binds the 2C protein of enterovirus 71 and is required for viral replication. *J. Biol. Chem. 282*, 5888–5898.
8. Dawson, T. R., Lazarus, M. D., Hetzer, M. W., and Wente, S. R. (2009) ER membrane-bending proteins are necessary for de novo nuclear pore formation. *J. Cell. Biol. 184*, 659–675.
9. Di Sano, F., Fazi, B., Citro, G., Lovat, P. E., Cesareni, G., and Piacentini, M. (2003) Glucosylceramide synthase and its functional interaction with RTN-1C regulate chemotherapeutic-induced apoptosis in neuroepithelioma cells. *Cancer Res. 63*, 3860–3865.
10. Steiner, P., Kulangara, K., Sarria, J. C., Glauser, L., Regazzi, R., and Hirling, H. (2004) Reticulon 1-C/neuroendocrine-specific protein-C interacts with SNARE proteins. *J. Neurochem. 89*, 569–580.
11. Melino, S., Nepravishta, R., Bellomaria, A., Di Marco, S., and Paci, M. (2009) Nucleic acid binding of the RTN1-C C-terminal region: toward the functional role of a reticulon protein. *Biochemistry 48*, 242–253.
12. Fazi, B., Melino, S., De Rubeis, S., Bagni, C., Paci, M., Piacentini, M., and Di Sano, F. (2009) Acetylation of RTN-1C regulates the induction of ER-stress via inhibition of HDAC activity in neuroectodermal tumours. *Oncogene 28*, 3814–3824.
13. Roth, S. Y., Denu, J. M., and Allis, C. D. (2001) Histone acetyltransferases. *Annu. Rev. Biochem. 70*, 81–120.
14. Marks, P. A., Miller, T., and Richon, V. M. (2003) Histone deacetylases. *Curr. Opin. Pharmacol. 3*, 344–351.
15. Takemura, R., Okabe, S., Umeyama, T., Kanai, Y., Cowan, N. J., and Hirokawa, N. (1992) Increased microtubule stability and alpha tubulin acetylation in cells transfected with microtubule-associated proteins MAP1B, MAP2 or tau. *J. Cell Sci. 103* (Part 4), 953–964.
16. Bannister, A. J., Miska, E. A., Gorlich, D., and Kouzarides, T. (2000) Acetylation of importin-alpha nuclear import factors by CBP/p300. *Curr. Biol. 10*, 467–470.
17. Marks, P., Rifkind, R. A., Richon, V. M., Breslow, R., Miller, T., and Kelly, W. K. (2001) Histone deacetylases and cancer: causes and therapies. *Nat. Rev. Cancer 1*, 194–202.
18. Dixon, J. W., and Sarkar, B. (1974) Isolation, amino acid sequence and copper(II)-binding properties of peptide (1−24) of dog serum albumin. *J. Biol. Chem. 249*, 5872–5877.
19. Laussac, J. P., and Sarkar, B. (1984) Characterization of the copper-(II)- and nickel(II)-transport site of human serum albumin. Studies of copper(II) and nickel(II) binding to peptide 1−24 of human serum albumin by ^{13}C and ^{1}H NMR spectroscopy. *Biochemistry 23*, 2832–2838.
20. Lau, S. J., Kruck, T. P., and Sarkar, B. (1974) A peptide molecule mimicking the copper(II) transport site of human serum albumin. A comparative study between the synthetic site and albumin. *J. Biol. Chem. 249*, 5878–5884.
21. Long, E. C. (1999) Ni(II),Xaa-Xaa-His metallopeptides DNA/RNA interactions. *Acc. Chem. Res. 32*, 827–835.
22. Kimoto, E., Tanaka, H., Gyotoku, J., Morishige, F., and Pauling, L. (1983) Enhancement of antitumor activity of ascorbate against Ehrlich ascites tumor cells by the copper:glycylglycylhistidine complex. *Cancer Res. 43*, 824–828.
23. Mack, D. P., and Dervan, P. B. (1990) Nickel-mediated sequence-specific oxidative cleavage of DNA by a designed metalloprotein. *J. Am. Chem. Soc. 112*, 4604–4606.
24. Harford, C., and Sarkar, B. (1997) Amino terminal Cu(II)- and Ni(II)-binding (ATCUN) motif of proteins and peptides: metal binding, DNA cleavage, and other properties. *Acc. Chem. Res. 30*, 123–130.
25. Jin, Y., and Cowan, J. A. (2005) DNA cleavage by copper-ATCUN complexes. Factors influencing cleavage mechanism and linearization of dsDNA. *J. Am. Chem. Soc. 127*, 8408–8415.
26. Brittan, I. J., Huang, X., and Long, E. C. (1998) Selective recognition and cleavage of RNA loop structures by Ni(II)·Xaa-Gly-His metallopeptides. *Biochemistry 37*, 12113–12120.
27. Gokhale, N. H., and Cowan, J. A. (2005) Inactivation of human angiotensin converting enzyme by copper peptide complexes containing ATCUN motifs. *Chem. Commun.* (*Cambridge*), 5916–5918.
28. Gokhale, N. H., and Cowan, J. A. (2006) Metallopeptide-promoted inactivation of angiotensin-converting enzyme and endothelin-converting enzyme 1: Toward dual-action therapeutics. *J. Biol. Inorg. Chem. 11*, 937–947.
29. Gokhale, N. H., Bradford, S., and Cowan, J. A. (2007) Stimulation and oxidative catalytic inactivation of thermolysin by copper.Cys-Gly-His-Lys. *J. Biol. Inorg. Chem. 12*, 981–987.
30. Krezel, A., Lesniak, W., Jezowska-Bojczuk, M., Mlynarz, P., Brasun, J., Kozlowski, H., and Bal, W. (2001) Coordination of heavy metals by dithiothreitol, a commonly used thiol group protectant. *J. Inorg. Biochem. 84*, 77–78.
31. LePecq, J. B., and Paoletti, C. (1967) A fluorescent complex between ethidium bromide and nucleic acids. Physical-chemical characterization. *J. Mol. Biol. 27*, 87–106.
32. Hoffmann, K., Brosch, G., Loidl, P., and Jung, M. (1999) A non-isotopic assay for histone deacetylase activity. *Nucleic Acids Res. 27*, 2057–2058.
33. Sigel, H., and Martin, B. (1982) Coordinating properties of the amide bond. Stability and structure of metal complexes of peptides and related ligands. *Chem. Rev. 82*, 385–426.
34. Appleton, D. W., and Sarkar, B. (1971) The absence of specific copper(II)-binding site in dog albumin. A comparative study of human and dog albumins. *J. Biol. Chem. 246*, 5040–5046.
35. Pogni, R., Baratto, M. C., Busi, E., and Basosi, R. (1999) EPR and $O2^{\prime -}$ scavenger activity: Cu(II)-peptide complexes as superoxide dismutase models. *J. Inorg. Biochem. 73*, 157–165.
36. Fang, Y.-Y., Ray, B. D., Claussen, C. A., Lipkowitz, K. B., and Long, E. C. (2004) Ni(II)·Arg-Gly-His-DNA interactions: investigation into the basis for minor-groove binding and recognition. *J. Am. Chem. Soc. 126*, 5403–5412.
37. Jin, Y., Lewis, M. A., Gokhale, N. H., Long, E. C., and Cowan, J. A. (2007) Influence of stereochemistry and redox potentials on the single- and double-strand DNA cleavage efficiency of Cu(II) and Ni(II) Lys-Gly-His-derived ATCUN metallopeptides. *J. Am. Chem. Soc. 129*, 8353–8356.
38. Brown, K. C., Yang, S. H., and Kodadek, T. (1995) Highly specific oxidative cross-linking of proteins mediated by a nickel-peptide complex. *Biochemistry 34*, 4733–4739.
39. Allfrey, V. G., Faulkner, R., and Mirsky, A. E. (1964) Acetylation and methylation of histones and their possible role in the regulation of RNA synthesis. *Proc. Natl. Acad. Sci. U.S.A. 51*, 786–794.
40. Chiani, F., Di Felice, F., and Camilloni, G. (2006) SIR2 modifies histone H4-K16 acetylation and affects superhelicity in the ARS region of plasmid chromatin in Saccharomyces cerevisiae. *Nucleic Acids Res. 34*, 5426–5437.
41. Doenecke, D., and Gallwitz, D. (1982) Acetylation of histones in nucleosomes. *Mol. Cell. Biochem. 44*, 113–128.
42. Gregoretti, I. V., Lee, Y. M., and Goodson, H. V. (2004) Molecular evolution of the histone deacetylase family: functional implications of phylogenetic analysis. *J. Mol. Biol. 338*, 17–31.
43. Shogren-Knaak, M., Ishii, H., Sun, J. M., Pazin, M. J., Davie, J. R., and Peterson, C. L. (2006) Histone H4-K16 acetylation controls chromatin structure and protein interactions. *Science 311*, 844–847.
44. de Ruijter, A. J., van Gennip, A. H., Caron, H. N., Kemp, S., and van Kuilenburg, A. B. (2003) Histone deacetylases (HDACs): characterization of the classical HDAC family. *Biochem. J. 370*, 737–749.
45. Verdin, E., Dequiedt, F., and Kasler, H. G. (2003) Class II histone deacetylases: versatile regulators. *Trends Genet. 19*, 286–293.
46. Blander, G., and Guarente, L. (2004) The Sir2 family of protein deacetylases. *Annu. Rev. Biochem. 73*, 417–435.
47. Stadtman, E. R. (1990) Metal ion-catalyzed oxidation of proteins: biochemical mechanism and biological consequences. *Free Radical Biol. Med. 9*, 315–325.
48. Stadtman, E. R. (1993) Oxidation of free amino acids and amino acid residues in proteins by radiolysis and by metal-catalyzed reactions. *Annu. Rev. Biochem. 62*, 797–821.
49. Khossravi, M., and Borchardt, R. T. (2000) Chemical pathways of peptide degradation. X: effect of metal-catalyzed oxidation on the solution structure of a histidine-containing peptide fragment of human relaxin. *Pharm. Res. 17*, 851–858.